SOME RECENT RESULTS ON CRACK-TIP ANALYSIS

K.C. HWANG and T.F. GUO

Department of Engineering Mechanics, Tsinghua University, Beijing 100084, China

ABSTRACT

In the 1st part, near-tip fields are constructed analytically for a quasi-static notch or crack growing in an elastic-creeping damaged materials. In some cases the relation between the crack growth rate and the loading parameter can be determined. The solutions degenerate into Hui & Riedel(1981)'s solution for undamaged material. In the 2nd part, crack-tip profiles for growing cracks in polymers are simulated numerically, and diverse patterns are observed.

KEYWOKDS

Creep damage, notch model, asymptotic field, crack tip superblunting.

1. INTRODUCTION

A study of asymptotic fields taking account of damage effects in fracture process zone is fundamental to deepen our understanding previously established through classical approach (Hwang, 1988). However, few results have been obtained due to the lack of correct formulations as well as the complexity of boundary value problems. It is known that the propagation of failure in damaged materials corresponds to a free boundary problem, and the failure front, a moving surface on which a specified rupture criterion is reached, gives rise to a crack in the sense of damage mechanics. Therefore, a notch (with a sharp notch angle undetermined) model (proposed by Guo, 1992) could reasonably describe the various failure fronts. Based on the notch formulations, different forms of asymptotic solutions for Kachanov-type creep damage materials (Kachanov, 1958; Hayhurst and Leckie, 1984) have been recently obtained by the present authors, which are constructed and classified according to the near-tip predominance analysis. The preliminary results are presented in the next section. Classical solutions of the problem with damage neglected were given by Hui and Riedel(1981).

In the above, cracks at critical state are conventionally assumed to propagate along a straight frontal path. The experiment observations on a loaded pre-existing crack prior to catastrophic growth, however, occasionally reveal the formation of intricate crack tip profiles, like superblunting (Fu et al.,1991) and crack tip branching (Ozmat et al.,1991). Little is known theoretically about different evolution patterns of crack tip profiles. The geometry of various crack tip profiles reflects the highly nonuniform deformation near the crack tip, and is critically dictated by the specific damage accumulation law linking to the material microstructure. Section 3 reviews the numerical simulation of crack tip profiles provided by Fu et al. for semi-crystalline polyproplene(PP) co-polymerized by high density polyethylene(HDPE) and further modified by SBS elastomers (Guo and Yang,1993; Yang et al.,1993). Five typical crack-tip profiles simulated are presented

herein which are featured by crack tip superblunting, branching, sharp notch and blunted notch with possible material detachment.

2. PROPAGATION OF FAILURE IN CREEP DAMAGE MEDIA

2.1. Constitutive equations for creep rupture. The evolution of damage with time is assumed to follow the law

$$\dot{\omega} = D[\kappa\sigma_1 + (1-\kappa)\sigma_e]^{\chi}(1+\varphi)^{-1}(1-\omega)^{-\varphi}, \tag{1}$$

and the damage effect on the stress / strain rate lies in

$$\dot{\varepsilon}_{ij} = \frac{1+\nu}{E}\dot{s}_{ij} + \frac{1-2\nu}{3E}\dot{\sigma}_{kk}\delta_{ij} + \frac{3}{2}B\sigma_e^{n-1}s_{ij}(1-\omega)^{-n} \tag{2}$$

where σ_1 is the maximum tensile principal stress, σ_e is the von Mises equivalent stress and s_{ij} is the stress deviator. In Eqs.(1) and (2),material constants are E(Young's modulus), ν(Poisson's ratio), B(the creep coefficient), D,n(the creep exponent), χ,φ and κ. Note that the constitutive equations remain valid until the specified rupture criterion, i.e., $\omega = 1$ or $\omega = \omega_f (0 < \omega_f < 1)$, is reached.

2.2. Notch model. Fig.1 shows the notch (with an angle $2\theta_d$ undetermined) geometry, where a Cartesian(x,y,z)-coordinate system with the z-axis lying along the failure front together with a velocity $\dot{a}$ in the positive x-direction. In this section, the so-called "continuity" ψ is used and is related to damage ω by $\psi = 1-\omega$.

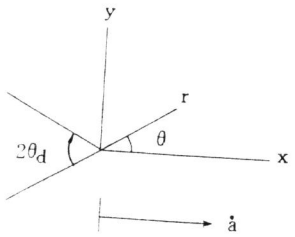

Fig.1. Notch geometry

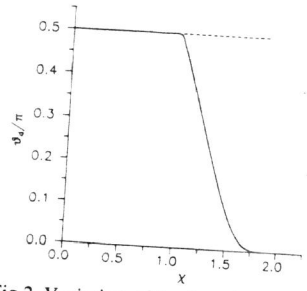

Fig.2. Variation of θ_d / π with χ

In accordance with the notch model, a seperated form of the continuity ψ and the stress σ_{ij} near the tip,

$$\psi \sim r^{\delta}\Psi(\theta), \quad \sigma_{ij} \sim r^{\gamma}T_{ij}(\theta) \tag{3}$$

is assumed where $\delta \geq 0$ and $\gamma < 0$ are required. It therefore follows that the notch half angle θ_d can be uniquely determined by supplementing the rupture criterion condition,

$$\lim_{r\to 0}\psi(r, \pm\theta = \pi - \theta_d) = \begin{cases} 0, & for\ \delta > 0 \\ \psi_f = 1-\omega_f > 0, & for\ \delta = 0 \end{cases} \tag{4}$$

Using Eqs.(1)-(4) and based on the usual small strain compatibility and static equilibrium equations, the analysis leads to the asymptotic stress and damage fields which are briefly reported

below, where only antiplane shear results are presented because of the limitation of space. For the case of antiplane shear, non-zero stress components are $\sigma_r = \sigma_{rz}$ and $\sigma_\theta = \sigma_{\theta z}$.

2.3. Asymptotic solutions for rupture criterion $\omega = 1$. When the asymptotic stress field near the notch tip is dominated by the elastic strain rates, we have (see Guo,1992)

$$\begin{bmatrix} \sigma_r(r,\theta) \\ \sigma_\theta(r,\theta) \end{bmatrix} = 2\Phi_0 r^{\gamma}(\gamma+1)\begin{bmatrix} sin(\gamma+1)\theta \\ cos(\gamma+1)\theta \end{bmatrix},$$

$$\psi(r,\theta) = \left\{\frac{[2\Phi_0(\gamma+1)(\kappa/\sqrt{3}-\kappa+1)]^{\chi}\overline{D}}{(1+\gamma\chi)\dot{a}}\right\}^{1/(1+\varphi)} r^{\delta}\Psi(\theta) \tag{5a}$$

with

$$\gamma = \frac{1}{2(1-\theta_d/\pi)} - 1 \equiv \gamma^L(\chi), \quad \delta = \frac{1+\gamma\chi}{1+\varphi}. \tag{5b}$$

In (5a) the factor Φ_0 is an unspecified factor and depends on the applied load and on the crack growth rate, $\overline{B} = (\sqrt{3})^{n+1}B$ and $\overline{D} = (\sqrt{3})^{\chi}D$. As $\theta_d \to 0$, $\gamma \to -1/2$, we have the degenerate case of elastic sharp crack and Φ_0 refers to local stress intensity factor. The angular distribution function of the continuity in (5) is the solution of the following one-order boundary value problem

$$\Psi^{1+\varphi}cos\theta - \frac{1}{1+\gamma\chi}(\Psi^{1+\varphi})'sin\theta = 1, \qquad \Psi(0) = 1,\ \Psi(\pi-\theta_d) = 0. \tag{6}$$

The prime denotes the derivative with respect to θ. The variation of θ_d / π with material parameter χ is plotted in Fig.2, where the solid and dashed lines represent the nontrivial and trivial ($\theta_d = \pi/2$) solutions of θ_d, respectively. Consequently, $\gamma^L(\chi)$ and δ can be easily computed from (5b). The asymptotic fields (5) remain valid if

$$[(1+\varphi)(n-1) - n\chi]\gamma^L(\chi) > n - (1+\varphi) \tag{7}$$

On the contrary, if material constants n,χ and φ satisfy such conditions as

$$n < 1+\varphi, \quad \chi < n-1, \quad \gamma^L(\chi) < \frac{n-(1+\varphi)}{(1+\varphi)(n-1)-n\chi} \tag{8a}$$

or

$$n > 1+\varphi, \quad \chi > n-1, \quad \gamma^L(\chi) > \frac{n-(1+\varphi)}{(1+\varphi)(n-1)-n\chi}, \tag{8b}$$

then elastic strain rates and creep rates have the same order of magnitude near the notch, and the stress and damage fields become

$$\sigma_i(r,\theta) = \alpha_n\left[\frac{\dot{a}}{[(G\overline{B})^{1+\varphi}/\overline{D}^n]^{1/(1+\varphi-n)}\cdot r}\right]^{-\gamma}T_i(\theta),$$
$$\psi(r,\theta) = \beta_n\left[\frac{\overline{D}^{n-1}/(G\overline{B})^{\chi}]^{1/(n-1-\chi)}\cdot r}{\dot{a}}\right]^{\delta}\Psi(\theta) \tag{9a}$$

where

$$\gamma = \frac{n-(1+\varphi)}{(1+\varphi)(n-1)-n\chi}, \quad \delta = \frac{n-1-\chi}{(1+\varphi)(n-1)-n\chi}, \tag{9b}$$

and the factors α_n and β_n are introduced to normalize $T_i(\theta)$ and $\Psi(\theta)$, respectively, i.e., $T_\theta(0) = 1$, $\Psi(0) = 1$. The subscript "n" denotes the dependence of α_n and β_n on n, χ, φ and κ. This field has the same feature of being independent of the remote loading and the prior history of crack growth as HR field (Hui and Riedel,1981). Only the current growth rate $\dot{a}$ and material parameters enter into (9). The angular distribution functions can be determined by a system of differential equations derived from the compatibility and damage evolution equations (see Guo and Hwang,1993), which will be not pursued here.

2.4. Asymptotic solutions for rupture criterion $\omega = \omega_f < 1$. For the rupture criterion $\omega_f < 1$, two forms of asymptotic solutions are also obtained as in subsection 2.3.
The case $\gamma^L(\chi) > -1/(n-1)$: For $\gamma^L(\chi) > -1/(n-1)$, the notch tip stress field is given by (5a), while the damage field is replaced by

$$\psi(r,\theta) = \psi_f + \frac{\overline{D}[2\Phi_0(\gamma^L+1)(\kappa/\sqrt{3}-\kappa+1)]^\chi}{(1+\varphi)\dot{a}\psi_f{}^\varphi(1+\gamma^L\chi)} \cdot r^{1+\gamma^L\chi}\Psi_1(\theta) \tag{10}$$

where Φ_0 and γ^L are the same as in (5), but the angular function $\Psi_1(\theta)$ is specified by the boundary value problem:

$$\Psi_1 cos\theta - \frac{1}{1+\gamma^L\chi}\Psi_1' sin\theta = 1, \qquad \Psi_1(0) = 0,\ \Psi_1(\pi-\theta_d) = 0. \tag{11}$$

Note that (11) and (6) have the same mathematical structure.
The case $\gamma^L(\chi) < -1/(n-1)$ and $\chi < n-1$: In this case, we have

$$\sigma_i(r,\theta) = \alpha_n\left(\frac{\dot{a}\psi_f{}^n}{\overline{GBr}}\right)^{1/(n-1)} T_i(\theta),$$

$$\psi(r,\theta) = \psi_f + \frac{[(\kappa/\sqrt{3}-\kappa+1)\alpha_n]^\chi}{(1+\varphi)[1-\chi/(n-1)]\dot{a}\psi_f{}^\varphi}\left(\frac{\dot{a}\psi_f{}^n}{\overline{GBr}}\right)^{\chi/(n-1)}\overline{Dr}\Psi_1(\theta). \tag{12}$$

As in (9),the factor α_n is introduced here to normalize $T_i(\theta)$. $\Psi_1(\theta)$ in (12) can be obtained by solving the following equations

$$\Psi_1 cos\theta - \frac{1}{1-\chi/(n-1)}\Psi_1' sin\theta = T^\chi(\theta), \qquad \Psi_1(0) = 1,\ \Psi_1(\pi-\theta_d) = 0 \tag{13}$$

where $T(\theta) = \sqrt{T_r^2(\theta) + T_\theta^2(\theta)}$ is the angular function of the equivalent shear stress. For convenience, the solutions (5),(9),(10) and (12) correspond to the cases named LE_2,E_1E_2,LF and E_1F, respectively in the work by Guo (1992). It is obvious that the well-known Hui-Riedel solution for undamaged materials (elastic nonlinear viscous materials) follows as a special case of E_1F case solution.

2.5. The crack growth rate. Under small scale yielding conditions, the creep crack growth rate can be evaluated according to the present E_1E_2 and E_1F cases of solutions. Matching at $\psi(r,\theta=0) = 1$the solutions and the elastic singular field characterized by the stress intensity factor K_{III}, one has the growth rate

$$\dot{a} = I_n\left(\frac{\overline{D}}{\overline{GB}}\right)^{(n-3)/(n-1-\chi)} G\overline{B}K_{III}{}^2 \tag{14a}$$

where I_n is an integration factor and is defined by

$$I_n{}^{-1} = \begin{cases} 2\pi\alpha_n^2/\beta_n{}^{\frac{(1+\varphi)(n-3)+n(2-\chi)}{n-1-\chi}}, & for\ E_1E_2 \\ 2\pi\alpha_n^2\left[\dfrac{(1+\varphi)(1-\chi/(n-1))(1-\psi_f)}{[(\kappa/\sqrt{3}-\kappa+1)\alpha_n]^\chi\psi_f}\right]^{(n-3)/(n-1)} \cdot \psi_f{}^{\frac{(1+\varphi)(n-3)+n(2-\chi)}{n-1-\chi}}, & for\ E_1F \end{cases} \tag{14b}$$

The results show that $\dot{a} \propto K_{III}^2$. Riedel (1990) has arrived at the same conclusion using self-similiar analysis.

3. DAMAGE INDUCED CRACK TIP PROFILES

3.1. Damage modelling. Taking into account of the deterioration effects on polymers by plastic flow, stress triaxiality and initial draw direction(IDD), a damage evolution law could be expressed as

$$\dot{\omega} = R(\overline{\mathbf{S}},\theta)\dot{\bar{\varepsilon}}^p, \quad R = A f(\theta) exp\left(\frac{3\bar{\sigma}_m}{2\bar{\sigma}}\right) \tag{15a}$$

where $\bar{\sigma}$ and $\bar{\sigma}_m$ denotes the J_2 flow stress and the mean hydrostatic stress, respectively and θ characterizes the inclination angle between the maximum deformation rate and IDD. The function $R(\overline{\mathbf{S}},\theta) = d\omega/d\bar{\varepsilon}^p$ is referred to as damage rate modulus, and the amplitude factor A is inversely proportional to the failure (logrithmic) strain $\bar{\varepsilon}_f^p$ when fibrillated chains reach their limit stretching ratio. The orientation fuction $f(\theta)$ in (15a) describing the damage anisotropy induced by IDD and normalized as unity for the degenerate case of damage isotropy, is defined as

$$f(\theta) = 2\frac{cos^2 2\theta + (1-\xi)sin^2 2\theta}{\eta cos 2\theta + \sqrt{(1-\xi)[4-(4\xi+\eta^2)sin^2 2\theta]}} \tag{15b}$$

where two dimensionless anisotropic damage parameters ξ and η are incorporated in (15b). ξ denotes the anisotropy of Hill's type which measures the relative damage contributions between chain rupture and chain shear, while η gives rise to the Bauchinger type anisotropy (see Guo and Yang, 1993).
In a combined hyperelastic and viscoplastic framework at finite deformation (Moran et al., 1990), one has the following constitutive formulations

$$\overline{\mathbf{S}} = (1-\omega)[\lambda_0 log(detF^e)\overline{\mathbf{C}}^{-1} + \mu_0(\mathbf{I} - \overline{\mathbf{C}}^{-1})], \tag{16a}$$

$$\overline{\mathbf{D}}^p = \dot{\bar{\varepsilon}}^p\left(\frac{3}{2\bar{\sigma}}\overline{\mathbf{C}}\cdot\overline{\mathbf{S}}'\cdot\overline{\mathbf{C}}\right) \tag{16b}$$

where λ_0 and μ_0 are Lame elastic constants in the reference configuration. $\overline{C} = \mathbf{F}^{eT}\cdot\mathbf{g}\cdot\mathbf{F}^e$ is the elastic right Cauchy-Green deformation tensor with $\mathbf{F}^e$ being defined by a multiplicative decomposition of the deformation gradient $\mathbf{F}$, and gbeing the covariant metric tensor, $\overline{\mathbf{S}}'$ is the deviatoric part of the symmetric second Piola-Kirchhoff stress tensor $\overline{S}$, and $\overline{\mathbf{D}}^p$ the plastic deformation rate with isotropic hardening which are all described in the intermediate configuration. The plastic strain rate $\dot{\bar{\varepsilon}}^p$ is written as

$$\dot{\bar{\varepsilon}}^p = \dot{\varepsilon}_0[(\bar{\sigma}/H(\bar{\varepsilon}^p,\omega)\ )^m - 1], \quad \bar{\sigma} \geq H(\bar{\varepsilon}^p,\omega) \tag{17a}$$

where

$$H(\bar{\varepsilon}^p,\omega) = (1-\omega)\sigma_0(1+\bar{\varepsilon}^p/\varepsilon_0)^N \tag{17b}$$

is a hardening function with exponent N, σ_0 is the reference stress, ε_0 and $\dot{\varepsilon}_0$ are reference strain and strain rate, respectively and m is the rate sensitivity exponent.

3.2. Numerical simulation. For the quadrilateral isoparametric elements to accommodate the $\bar{B}$-bar method for near-incompressible deformation (Moran et al., 1990), the element failure criterion is phrased in an averaging sense. The element damage evolution can be written as

$$\dot{\Omega} = \frac{1}{V^e}\int_{V^e} \dot{\omega} dV \tag{18}$$

where V^e is the element volume in the reference configuration. The element damage increment $\triangle\Omega$ in a load step relates to the increment of effective plastic strain $\triangle\bar{\varepsilon}^p$ by the following explicit algorithm

$$\triangle\Omega = \{\sum_i^{NINT} J_i H_i [R(\bar{\mathbf{S}}_{n+1},\theta_{n+1})\triangle\bar{\varepsilon}^p]_i\} / \{\sum_i^{NINT} J_i H_i\} \tag{19}$$

where NINT is the Gaussian integration points within an element, J_i and H_i are the Jacobian and weight coefficient of the i-th Gaussian point, respectively. After obtaining $\triangle\Omega$, one can update the element damage by

$$\Omega_{n+1} = \Omega_n + \triangle\Omega \tag{20}$$

The subscripts "n" and "n+1" refer to the instants of t_n and t_{n+1}, respectively. In the numerical calculation, the complete failure of the element is defined by $\Omega = 0.99$, from which the corresponding nodal force will be released in a number of loading steps.

The present damage theory enables us to simulate numerically the crack tip profiles for both plane strain small scale yield (SSY) and single edge cracked panel (SECP) geometries. Five typical crack tip profiles, generated by different settings of anisotropic damage parameters (see Guo and Yang, 1993), are reproduced here. The simulated crack tip superblunting and branching are shown in Fig.3, and the corresponding contour plots of damage fields are furnished in Fig.4. The mesh deformation shown in Fig.5 provides another two crack tip profiles of trident shape damage channeling and sharp notch. The global deformation of the SECP mesh is shown in Fig.6a, and the amplified inner layers in Fig.6b near the crack tip reveal a blunted notch tip profile and material detachment.All the five profiles were experimentally actually observed.

REFERENCES

Fu, Z., S.Shi, Y.Sun and W.Yang (1991), Fracture Process Zone and Toughening Model of Modified Polypropylene Multiphase Systems, *China Plastics*, Vol.5, No.2, 12–19.

Guo, T.F. (1992), The Damage Process Zone around a Crack Tip, Ph.D. Thesis, Dep. Engng. Mech., Tsinghua University, Beijing, China.

Guo T.F. and K.C. Hwang (1993), The Propagation of Failure in Creeping Damage Materials, submitted for publication.

Guo, T.F. and W.Yang (1993), Crack Tip Profiles Generated by Anisotropic Damage, to appear in *Int. J. Damage Mech.*, vol.3.

Hayhurst, D.R. and F.A. Leckie (1984), In: Mechanical Behaviour of Materials, *Proc. of ICM4* (J. Carlsson and N.G. Ohlson, eds.), Vol.2, 1195–1212, Pergamon Press, Oxford.

Hui, C.Y. and H. Riedel (1981), The Asymptotic Stress and Strain Field near the Tip of a Growing Crack in Creep Conditions, *Int. J. Fracture*, Vol.17, 409–425.

Hwang, K.C. (1988), Damage and Fracture, In: Advances in Plasticity (R. Wang et al., eds.), Chapter 2, China Railway Press, Beijing.

Kachanov, L.M. (1958), On the Rupture-Time under Creep, *Izv. Akademii Nauk SSSR*, Vol.8, 26–31.

Moran, B., M. Ortiz and C.F. Shih (1990), Formulation of Implicit Finite Element Methods for Multiplicative Finite Deformation Plasticity, *Int. J. Num. Method Engng.*, Vol.29, 483–514.

Ozmat, B., A.S. Argon and D.M. Parks, (1991), Growth Modes of Cracks in Creeping Type 304 Stainless Steel, *Mech. Mater.*, Vol.11, 1–17.

Riedel, H. (1990) Creep Crack Growth under Small-Scale Creep Conditions, *Int. J. Fracture*, Vol.42, 173–188.

Yang, W., T.F. Guo and Z.L. Fu (1993), Crack Tip Superblunting: Experiment, Theory and Numerical Simulation, *Acta Mechanica Sinica*, Vol. 9.

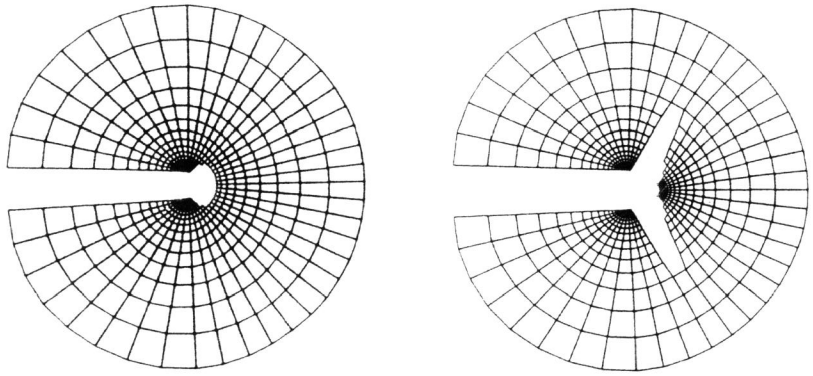

(a) (b)

Fig.3. Crack tip superblunting (a) and branching (b).

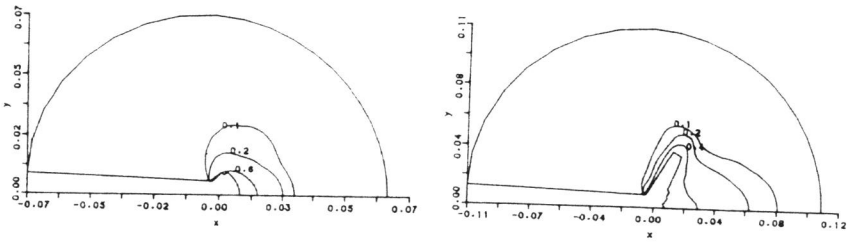

(a) (b)

Fig.4. Contour plots of damage ω near the crack tips of superblunting (a) and branching (b).

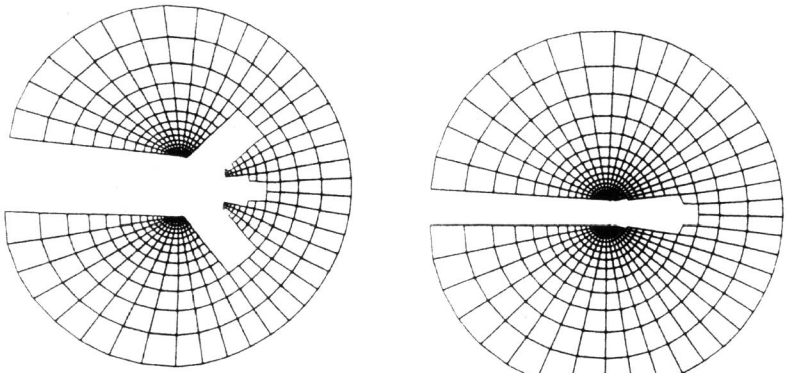

(a) (b)

Fig.5. Trident crack tip profile (a) and sharp notch tip profile (b).

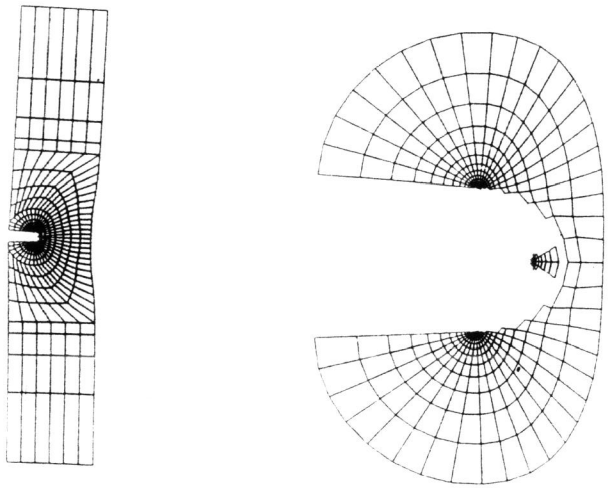

(a) (b)

Fig.6 Blunted notch tip profile. (a) global deformation of SECP; (b) amplified inner layers to reveal blunted notch tip and material detachment.